



# Numerical Prediction of Experimentally Observed Behavior of a Scale Model of an Offshore Wind Turbine Supported by a Tension-Leg Platform

## Preprint

I. Prowell  
*MMI Engineering*

A. Robertson and J. Jonkman  
*National Renewable Energy Laboratory*

G. M. Stewart  
*University of Massachusetts*

A. J. Goupee  
*University of Maine*

*To be presented at the 2013 Offshore Technology Conference  
Houston, Texas  
May 6-9, 2013*

**NREL is a national laboratory of the U.S. Department of Energy, Office of Energy Efficiency & Renewable Energy, operated by the Alliance for Sustainable Energy, LLC.**

**Conference Paper**  
NREL/CP-5000-57615  
January 2013

Contract No. DE-AC36-08GO28308

## NOTICE

The submitted manuscript has been offered by an employee of the Alliance for Sustainable Energy, LLC (Alliance), a contractor of the US Government under Contract No. DE-AC36-08GO28308. Accordingly, the US Government and Alliance retain a nonexclusive royalty-free license to publish or reproduce the published form of this contribution, or allow others to do so, for US Government purposes.

This report was prepared as an account of work sponsored by an agency of the United States government. Neither the United States government nor any agency thereof, nor any of their employees, makes any warranty, express or implied, or assumes any legal liability or responsibility for the accuracy, completeness, or usefulness of any information, apparatus, product, or process disclosed, or represents that its use would not infringe privately owned rights. Reference herein to any specific commercial product, process, or service by trade name, trademark, manufacturer, or otherwise does not necessarily constitute or imply its endorsement, recommendation, or favoring by the United States government or any agency thereof. The views and opinions of authors expressed herein do not necessarily state or reflect those of the United States government or any agency thereof.

Available electronically at <http://www.osti.gov/bridge>

Available for a processing fee to U.S. Department of Energy and its contractors, in paper, from:

U.S. Department of Energy  
Office of Scientific and Technical Information  
P.O. Box 62  
Oak Ridge, TN 37831-0062  
phone: 865.576.8401  
fax: 865.576.5728  
email: <mailto:reports@adonis.osti.gov>

Available for sale to the public, in paper, from:

U.S. Department of Commerce  
National Technical Information Service  
5285 Port Royal Road  
Springfield, VA 22161  
phone: 800.553.6847  
fax: 703.605.6900  
email: [orders@ntis.fedworld.gov](mailto:orders@ntis.fedworld.gov)  
online ordering: <http://www.ntis.gov/help/ordermethods.aspx>

Cover Photos: (left to right) PIX 16416, PIX 17423, PIX 16560, PIX 17613, PIX 17436, PIX 17721



Printed on paper containing at least 50% wastepaper, including 10% post consumer waste.

# Numerical Prediction of Experimentally Observed Behavior of a Scale-Model of an Offshore Wind Turbine Supported by a Tension-Leg Platform

I. Prowell, MMI Engineering; A. Robertson, J. Jonkman, National Renewable Energy Laboratory; G.M. Stewart, University of Massachusetts; A.J. Goupee, University of Maine

---

## Abstract

Realizing the critical importance the role physical experimental tests play in understanding the dynamics of floating offshore wind turbines, the DeepCwind consortium conducted a one-fiftieth-scale model test program where several floating wind platforms were subjected to a variety of wind and wave loading conditions at the Maritime Research Institute Netherlands (MARIN) wave basin. This paper describes the observed behavior of a tension-leg support platform (TLP), one of three platforms tested, and the systematic effort to predict the measured response with the FAST simulation tool using a model primarily based on consensus geometric and mass properties of the test specimen. The initial model was tuned through adjusting damping and stiffness of the platform and tower using free-response test results.

Simulation results showed reasonable agreement with the experimental data for most quantities, including platform surge, tower-base bending moment, and tendon tension across a broad range of tests. Of particular note was the under prediction of platform-pitch acceleration for most scenarios investigated. In light of past findings for TLP pitch behavior, it was hypothesized that second-order sum-frequencies present in the experiment and not considered numerically were at least partially responsible for this error. For experimental conditions that led to slack-line events in the wave basin, FAST simulations sometimes predicted corresponding events. The prediction of the slack-line events and numerical stability of the following dynamic response was encouraging. However, multiple experimental tests showed slack-line events that were not predicted numerically. In particular, the FAST simulations failed to predict slack-line events that occurred while the rotor was stationary. It is believed that under prediction of wind drag on the tower, the exposed portion of the platform, and possibly the rotor was the primary cause for this modeling error. Increasing the accuracy for the pitch response would improve prediction of slack-line events.

It is suggested that the following efforts be made to improve FAST's predictive capabilities for turbines supported on floating platforms: 1) Allow specification of platform geometries other than a constant diameter cylinder for the computation of hydrodynamic forces. The need for adjustments to damping would likely decrease if the geometry of the TLP were modeled explicitly (e.g. the larger diameter portion near the bottom of the platform and the platform legs); 2) Implement a dynamic model of the platform tendons so that contributions beyond cable tension are more explicitly considered; 3) Consider second-order hydrodynamics that are believed to be a source of error in the prediction of the platform pitch; and 4) Develop wave loading routines for FAST that more readily allow for reproduction of the experimentally observed wave time history instead of only matching the wave spectrum, similar to how a variable wind time history can be explicitly defined.

Further, future wave tank tests for a TLP supported floating turbine should consider: 1) additional instrumentation to ascertain tower mode shapes to assist in classification of resonant frequencies as specific mode types; 2) the importance of the pitch response of a TLP and how to accurately quantify the pitch response experimentally; 3) higher sampling rates to better capture the response of the tower-bending behavior that, for the tested TLP, appears to be highly coupled with platform dynamics; and 4) better scaling of rotor aerodynamics.

In light of potential improvements, results based on current simulation capabilities showed that a calibrated FAST model was, within a reasonable level of accuracy, able to predict many dynamic response quantities of a TLP-supported floating turbine under numerous loading scenarios.

## Introduction

Under the direction of the University of Maine, an experimental test was performed on a one-fiftieth-scale floating wind turbine model to investigate the behavior of three different floating platform concepts at the Maritime Research Institute Netherlands (MARIN). The one-fiftieth-scale turbine design was based on the National Renewable Energy Laboratory's (NREL) 5-MW reference turbine (Jonkman et al. 2009) with modifications required to accommodate construction at test scale. Detailed information regarding the model scale turbine is documented by Martin (2011). The turbine was placed on three different support platforms: a spar buoy, a semisubmersible, and a tension-leg platform (TLP). Summaries of experimental results from all three support platforms are available in Goupee et al. (2012) and Koo et al. (2012). Of the three platforms tested, the TLP was considerably lighterweight and would likely be more economical in terms of material costs, but not necessarily in anchoring costs. This manuscript details the test results for the TLP and does not address the results from the spar buoy or the semisubmersible. Figure 1 illustrates the turbine test configuration. The paper presents a more in-depth analysis of the preliminary TLP results published by Stewart et al. (2012). Specifically, the model developed by Stewart is further refined, scenarios for more simulations are presented, and quantities predicted numerically by the FAST tool (Jonkman and Buhl 2005) and those observed experimentally are compared.

## Experimental Setup and Conventions

The test turbine represents turbines under consideration for near-term deployment to deepwater sites where a floating platform is required. Pertinent details of the model scale turbine are presented in Table 1. In many respects the scaled properties of the tested turbine departs significantly from the 5-MW NREL reference turbine. Though tested at one-fiftieth scale, all results presented here are translated to full scale using similitude laws (Jain et al. 2012) for ease of interpretation. A summary of the platform parameters is shown in Table 2.

For reference, the coordinate convention used herein is illustrated in Figure 2. Translation of the platform is referred to as surge, sway, and heave, which are in the X, Y, and Z directions, respectively. For platform rotation, the terms roll, pitch, and yaw are used to represent positive right-handed rotation about each of the X, Y, and Z axes, respectively.

## Dynamic Properties of Physical Turbine Model

Impulse-response experiments were performed on the turbine by hitting the structure with a hammer, both while connected to a very rigid base (mimicking a land-based support) and also while supported by each of the three floating platforms. The turbine was struck in both the X and Y directions at the water level, 25 m above the water level, and 92.5 m above the water level. An additional strike was performed in the vertical (Z) direction at 25 m above water level. The hammer used in the tests was not instrumented and, as a result, only output quantities are available for analysis. Analyses of hammer tests are presented by Martin (2011) and de Ridder et al. (2011b; 2011a). For the rigid-base tests, Martin found a natural frequency of 0.29 Hertz (Hz) for the tower's primary bending mode in the fore-aft and side-to-side directions. The second fore-aft natural frequency identified by Martin on the rigid platform is 1.24 Hz. When placed on the TLP, little change was observed by Martin in the frequency of the tower's primary fore-aft (0.28 Hz) and side-to-side modes (0.29 Hz). The second fore-aft frequency was reported as 1.16 Hz. De Ridder et al. (de Ridder et al. 2011b) only reported the first fore-aft natural frequency with a slightly lower value of 0.274 Hz when on the rigid support and 0.267 Hz when supported by the TLP. Full plots of the TLP hammer tests that showed results beyond the primary bending mode of the tower were presented by de Ridder et al. (de Ridder et al. 2011a), but no interpretation was provided. It appears that peak picking from the power spectrum was used by both Martin and de Ridder et al. to develop reported results.

To gain further insight from the hammer tests, the frequency-domain-decomposition (FDD) algorithm (Brincker et al. 2000) was used to clarify modes that may not have been identified by peak picking. For the hammer tests, the instrumentation used was a limited subset of that used in the other tests and was recorded at 141.4 Hz instead of 14.14 Hz. For consistency between instruments, only translational accelerometers placed along the tower were used in the analysis presented here. Three channels for the low and mid accelerometers (Figure 3) were recorded and available for the tests, which results in a total of six channels. The limited number of channels, in particular only one accelerometer on the flexible portion of the tower, presents a challenge in identifying the modes of the turbine when supported on the TLP. It is typical that the number of modes capable of being identified is limited to the number of channels. Using insight gained from the FAST model of the TLP supported turbine, additional modes were inferred. Results are summarized in Table 3 with data processing such that the minimum frequency step resolved was 0.004 Hz. Differences between the results reported here and those in the past will be addressed later in this manuscript.

## Calibration of the FAST Model

As reported and clearly demonstrated in Stewart et al. (2012), a FAST model of the TLP-supported turbine simply based on scaled-design specifications for the model of the rotor, nacelle, tower, and platform (Martin 2011; de Ridder et al. 2011b; de Ridder et al. 2011a) produces results that diverge significantly from those observed in the wave tank. This divergence was also present in the spar and semisubmersible results. To reduce the discrepancies and gain more in-depth insight from the experimental results, investigations using the DeepCwind data have adopted the approach of adjusting the numerical model to more accurately recreate observed test results for a small subset of the tests. This tuning was justified as a preliminary way to account for unknown data and to include the effects of physics, such as the viscous drag on the platform legs, that are not explicitly modeled numerically. In this investigation two main properties, damping and stiffness, for the platform degrees of freedom (DOFs) were adjusted to approximate the influence of unmodeled physics and possibly account for other modeling limitations, such as material properties. In addition, component mass, stiffness, and aerodynamic properties were adjusted as deemed appropriate (Martin 2011, Stewart et al. 2012).

Because the tendons are critically important to the response of a TLP, it was decided to first determine the appropriate platform displacement that best recreated the experimentally reported tendon tension. For the DeepCwind TLP, MARIN reports a displacement of 2,840 metric tons (de Ridder et al. 2011b), which for an assumed water density of 1,025 kilograms per meter cubed ( $\text{kg/m}^3$ ), is equivalent to a displaced volume of 2,770  $\text{m}^3$ . In processing the experimental data, tendon tension for each test was zeroed to remove sensor drift, and a static value was added from an early calibration test (de Ridder et al. 2011b). The static values vary from a minimum of 4,697.6 kilonewtons (kN) for tendon 1 (downwind, positive X), 4,754.9 kN for tendon 2 (upwind, positive Y), and a maximum of 4,813.3 kN for tendon 3 (upwind, negative Y). However, due to the symmetry of the numerical model when simulated in the FAST tool, tendons 2 and 3 show identical tensions when the turbine is at rest. Due to this discrepancy between the numerical and experimental results, instead of trying to match the individual tendon tension, the average tension was matched. To accomplish this, platform displacement was iteratively altered so that the average line tension matched the average line tension observed experimentally. The resulting value of displaced volume of 2748.8  $\text{m}^3$  was adopted. This change represents less than a 1% reduction in the displaced volume. This small discrepancy is possibly due to measurement error or other discrepancies between the idealized configuration and the actual test configuration.

Free-decay tests were conducted that focused on identifying the frequencies and decay rates of the six DOFs: surge, sway, heave, roll, pitch, and yaw. By applying additional damping and stiffness to each of the six platform DOFs, these test results provided the body of information used to calibrate the FAST turbine model. Past efforts to calibrate the TLP model focused on adding damping that was linearly proportional to the velocity for each DOF (Stewart et al. 2012). More detailed investigation of the damping for each platform DOF, however, showed amplitude dependence. The upper portion of Figure 4 shows the time trace of the experimentally recorded platform-surge displacement in blue for a surge free-decay test. In the lower portion, the log-decrement method is used to estimate the approximate damping ratio for each successive cycle. The experimental results clearly show amplitude dependence for the damping. Similar to that assumed in the Morison Equation, a drag term that is proportional to the velocity squared was added for each of the platform DOFs to approximate the drag behavior observed in the test data.

The platform-heave natural frequency was used to calibrate the tendon axial stiffness. Initial models used a value of 7,500 meganewtons (MN) for the cross-sectional stiffness of each tendon (de Ridder et al. 2011b). However with the fixed system mass and displacement specified above and the specified stiffness, the resulting heave frequency was approximately 1 Hz (Stewart et al. 2012). Experimental results showed a heave frequency closer to 0.86 Hz (Table 3). The discrepancy is possibly caused by compliance introduced by the force gauges used to measure tendon tension. To match the observed frequency, the tendon stiffness was reduced to 6,118 MN. Additionally, to reduce initial heave transients, the unstretched tendon length was slightly modified from the specified value of 171.4 m to 171.36 m. After adjusting the tendon stiffness and unstretched length, the added damping was iteratively adjusted. In the final model, a value of 0 was used for additional linear damping and a value of 2.5  $\text{MNs}^2/\text{m}^2$  was used for quadratic damping. This additional quadratic damping likely represents energy dissipation of the unmodeled viscous drag from the platform legs and larger diameter portion of the platform moving vertically in the water.

Following calibration of the platform tendons for tension and heave vibration characteristics, the other platform DOFs were calibrated in a similar manner to match experimentally recorded free-response tests. A summary of the required adjustments are presented in Table 4. An example of the resulting match for the free-decay surge test is provided in Figure 4. Visual inspection of the recreated time history (red) shows it is almost identical to that recorded in the wave tank (blue). The damping estimates from the model and the experiment differ more significantly than the time histories, but recreate the approximate damping levels across a range of displacements with results diverging slightly for large amplitudes.

The tower mode shapes required by FAST were generated in BModes (Bir 2005) using the properties derived for the calibrated platform mass and stiffness characteristics, hydrodynamic added mass and hydrostatic restoring properties from a WAMIT model (WAMIT Inc. 2006), and mass and stiffness properties of the turbine tower and mooring system. After removing the translation and rotation at the tower base as required by FAST (Figure 5), the mode shapes predicted by BModes were able to be accurately approximated as a 6<sup>th</sup>-order polynomial for direct use in the FAST model. Table 3 presents a summary of the modal frequencies predicted by the calibrated model and those observed experimentally.

For illustrative purposes, the mode shapes predicted at 0.267 Hz and 1.30 Hz are presented in Figure 6 and Figure 7. These two frequencies both contain tower fore-aft bending and platform-pitch contributions. In past publications, these two modes have been interpreted in various combinations as tower 1<sup>st</sup> fore-aft bending, platform pitch, and tower 2<sup>nd</sup> fore-aft bending. The figures clearly illustrate the high degree of coupling between tower bending and platform rotation in the overall turbine dynamics that has made interpretation of these modes difficult. Investigation of the mode shape at 1.30 Hz (Figure 7) shows that the tower is in single curvature, which supports the interpretation of a beam 1<sup>st</sup> bending mode in which the boundary conditions resemble a free-free condition instead of a fixed-free condition. Based on the extremely low frequencies for surge and sway, it is clear that translation of the tower base more closely resembles a free condition, but conclusions about the rotational fixity are not as clear and have contributed to variations in classification of modes (Koo et al. 2012). Because the mode shape at 1.30 Hz shows single curvature and is at a higher frequency than the fixed-base 1<sup>st</sup> fore-aft bending frequency (Martin 2011; de Ridder et al. 2011b), it is interpreted as the 1<sup>st</sup> fore-aft tower-bending frequency. The presence of a higher mode (3.236 Hz) that clearly shows double curvature in the tower (Figure 8) further supports this interpretation. Subsequently, the mode at 0.267 Hz is interpreted as platform pitch. Similar logic was employed in classification of the tower side-to-side and platform-roll modes.

### Simple Loading

Following hammer and free-response testing, the turbine was subjected to a number of loading scenarios. Initial scenarios focused on single-source loading from either wind or waves. A summary of the tests conducted for the wind-only load cases is reported in Table 5. Simulations in FAST were conducted that corresponded to the experimental test conditions for these tests, but wind speeds were altered slightly from those reported by de Ridder et al. (2011b) to more accurately simulate the measured experimental conditions. For each simulation, a total of approximately 43 minutes was simulated, but only the final 10-minute period was analyzed to ensure that transient behavior did not influence the reported results. The lengths of experimental tests varied, but for consistency in the results reported here, a 10-minute period was selected and used. For the wind-only tests, the primary quantity of interest was the force exerted on the system by the wind. Mean platform surge (Figure 9) and tower-bending moment (Figure 10) were the main measured quantities impacted by static wind forces. The MARIN and FAST data show a horizontal offset for display purposes and the FAST simulations occurred at the same wind speeds as the MARIN tests. Due to past efforts to calibrate airfoil properties for the tested turbine, simulation results showed good agreement with those observed experimentally (Martin 2011, Coulling et al. 2013a). Aerodynamic characteristics of the scaled model's rotor were one of the areas that differed most significantly from the 5-MW NREL reference turbine and the resulting rated wind speed was approximately 21 m/s instead of 12 m/s. This difference in aerodynamics resulted in higher wind speeds for specific rotor speeds than would be expected for the 5-MW reference turbine. It was noted that for the high wind condition (30.5 m/s)—when the blades were feathered and the rotor was not spinning—there was a more significant under prediction in terms of percentage of platform surge. The primary source of this discrepancy was likely due to the wind drag on the tower and exposed portion of the platform not being calculated in the FAST model. When the rotor was stationary and feathered, these forces contribute a larger fraction of the overall wind force on the turbine system. The trends observed for the wind-only simulations suggest that the wind force should be reasonably predicted for situations where the rotor was spinning but may be underestimated when the rotor was stationary.

A complementary set of tests were conducted in which loading consisted of only regular waves at a fixed period and magnitude. The parameters of the waves imparted are summarized in Table 6. As with the wind-only tests, a set of 43-minute simulations were run with corresponding load conditions. Reported results only contain information for the final 10-minute portion of the simulations after all initial transients had dissipated. As before, only a 10-minute portion of the experimental results were considered for comparison. Similar to the wind-only tests, the platform-surge statistics showed reasonable results (Figure 11). For the smaller sea states (1.92 m and 7.58 m), the predictions were of high quality but deteriorated as wave amplitude increased and the period elongated. The largest error, an approximately 25% under prediction, occurred for waves with a period of 20 s and a height of 11.12 m. However, platform-pitch acceleration, reported in Figure 12, was significantly under predicted by as much as a factor of 10 in many cases. Clearly, an underlying mechanism exciting pitch of the platform—likely second-order hydrodynamics—was not well captured in the FAST model (Coulling et al. 2013b). Other investigated parameters, including tendon tension, tower-bending moment, and platform heave, showed significantly better agreement.

An illustrative reproduction of representative platform-response plots is shown in Figure 13 and Figure 14. In the left portion of Figure 14, the differences in platform-pitch acceleration are shown. Though the experimental measurement visibly shows a noise floor that impedes a clear picture of the pitch response in comparison to the simulations, peaks are visible at two frequencies, the wave frequency (0.13 Hz) and the platform-pitch frequency (0.268 Hz). The predicted response shows reasonable correlation in amplitude at the wave frequency but underestimates the response at the platform-pitch frequency. This discrepancy can be partially explained by the presence of harmonics in the experimentally realized regular waves that were not present in the simulated waves, which leads to unsimulated excitation at the platform-pitch frequency. It was believed that, more generally, the under prediction of platform pitch can be attributed to second-order sum-frequency excitation. Past investigations have shown this phenomenon to be important in understanding the pitch response of a TLP (Naess and Ness 1992; Kim 1991). This is particularly true because typical pitch and roll frequencies of TLPs reside outside of the range of significant wave energy and are not directly excited. Second-order hydrodynamics may also contribute to the under prediction of platform surge for long period waves.

These simple load cases suggest that the turbine dynamics are reasonably recreated across many different independent wind and wave conditions, but appear to systematically underestimate extremes for investigated response quantities.

### Combined Loading for Normal Conditions

Of more interest than isolated wind or wave loading is combined wind and wave loading scenarios. Numerous wind and wave loading scenarios were conducted in the experiment as identified in Table 7. Here the results where the turbine was excited by a JONSWAP (Joint North Sea Wave Observation Project) spectrum while simultaneously being subjected to steady winds of different levels are presented. As before, numerical simulations were conducted for a total of approximately 43 minutes with the last 10-minute portion of the simulation used for the reported results to ensure transient behavior did not influence results. Similarly, the last 10-minute portion of the experimental response was selected by visual inspection for reported results. In addition, for these simulations, a user-defined wave spectrum was introduced in FAST to match the wave spectrum recorded experimentally. Though the realized wave time histories do not coincide, the difference between the wave power spectra was minimized through this approach. Figure 15 shows a comparison of the waves recorded in the tank as compared to those simulated for the test with 11.4-m/s winds and JONSWAP waves with a peak-spectral wave period ( $T_p$ ) of 12.1 s and significant wave height ( $H_s$ ) of 7.1 m. Both the time history and power spectra show good qualitative correlation. A summary of the quantitative statistics of the waves, presented in Figure 15, also shows reasonable agreement. Results for the presented cases should be viewed with consideration that differences in wave statistics will likely propagate to the turbine-response parameters. This was particularly true for the final scenario presented where the wave basin showed wave heights varying from -6.8 m to 7.8 m, but the FAST simulation only had waves varying from -6.2 m to 4.9 m.

For a TLP, tendon tension is of particular importance for design. Figure 16 presents a summary of the tension statistics for tendon 1 (the downwind tendon), which exhibited the largest variation among the tendons. Due to direct calibration of mean tendon tension and the dominance of the mean component in the magnitude, relatively good agreement was observed across most of the tests presented. However, the experimental tendon tension showed a negative value for the test with 21-m/s winds and a 7.1-m significant wave height, meaning that the tendon had gone slack. It is essential that slack-line events do not occur for a deployed system because the following force from the snap-back of the tendon will likely exceed the tendon, anchor, or fairlead capacity and create an impulse that will be propagated through the structure, exciting all of its Eigen frequencies. For a TLP with 3 legs like the one investigated here (which has no redundancy), such an event could cause complete loss of a realistic full-scale system. The FAST simulation for the corresponding scenario does not predict this negative tendon tension and the subsequent significant peak in tension.

Inspection of the slack-line event in the experimental time history clearly showed that it was in direct response to a significant wave. The specific wave sequence was a trough elevation of -6.8 m followed by a crest of 7.3 m and another subsequent trough of -6.1 m. Though the FAST wave power spectra showed a good match with the experimental power spectra, the most extreme comparable wave was a -6.1 m trough followed by a 4.8 m crest and a trough of -4.7 m. It is likely that if FAST were capable of directly recreating the large wave, the slack-line event would have been numerically predicted. For this reason, it is suggested that efforts be made to enable more direct simulation of an observed wave time history in FAST instead of simply matching the wave spectrum.

Again, platform-pitch acceleration (Figure 17) is significantly underestimated. The extent of underestimation is more significant than that for the regular wave tests. Figure 18 shows a typical comparison of the wave time history and power spectra from the wave tank and the simulation. Unlike the regular wave tests, where harmonics that were present in the wave tank were not recreated numerically, the power spectra showed good agreement across all platform frequencies. This suggests that some excitation mechanism was not being modeled numerically. Based on past findings (Naess and Ness 1992; Kim 1991) showing that second-order sum-frequency wave loads contribute significantly to the pitch response of a TLP, it was hypothesized that this was at least partially attributable to their omission in the simulation.

Despite the under prediction of platform-pitch acceleration across all tests and the lack of predicting the observed slack-line event in 21-m/s winds with 7.1-m waves, the FAST model did a good job predicting the character of the turbine response for many of the investigated parameters. Figure 19 and Figure 20 show the time histories and power spectra for some quantities of interest for the test with an 11.4-m/s wind speed and a 7.1-m significant wave height. These figures clearly show similar response characteristics for all time histories other than platform-pitch acceleration. Further, with consideration of the noise floor of the experimental instrumentation, which is clearly evident in the platform surge above 0.3 Hz, the power spectra match well. For frequencies above 0.4 Hz, results diverge more significantly than at lower frequencies.

### **Combined Wind and Wave Loading for Extreme Conditions**

Beyond normal operational scenarios, it is vital to be able to predict the extreme response of a structure. Table 8 presents parameters for what are considered survival conditions for the turbine. One scenario has the turbine operating in an extreme sea state and the other has the turbine rotor stationary in winds beyond the turbine cut-out wind speed. Statistics for the simulated wave conditions show better agreement with the experimental conditions (Figure 21) than those for the calmer sea states discussed above. Tendon 1 results for the wave tank clearly show slack-line events for both conditions (Figure 22). In the numerically simulated results, it was observed that a slack-line event was only predicted for the operational scenario. This lack of prediction of a slack-line event when the rotor was stationary can be partially justified by the under prediction of wind forces in such a scenario (Figure 9), which would cause the downwind tendon (tendon 1) tension to be overestimated. It is possible that improvements in prediction of wind forces for the stationary rotor condition would improve prediction of a slack-line event.

A qualitative comparison of the time histories and power spectra for the operational extreme test shows a better degree of correlation between the experimental results and numerical simulations (Figure 23 and Figure 24) than in calmer sea states. The time history of tendon 1 in the right portion of Figure 23 shows the slack-line event around 250 seconds. This event was responsible for both extremes seen in the experiment and the simulation in Figure 22. FAST showed reasonable correlation with the minima, but under predicts the snap-back of the line. The source of under prediction of the snap-back was unclear, but may be attributable to the lack of a dynamic model for the tendon, or possibly, the selected quadratic damping model over estimates the damping for platform pitch in such an extreme event. The power spectrum of the tension for tendon 1 showed that most of the contributing frequencies to the tendon tension were well modeled. Specifically, the wave excitation centered around 0.09 Hz, platform pitch at 0.268 Hz, and platform heave at 0.863 Hz. However, the contribution from tower first bending at 1.3 Hz was significantly underestimated by FAST. It is possible that the tower damping value selected, 2.1% for the first mode, was too high. However, significantly reducing the value to 0.5% made little difference.

It is interesting to observe the platform-pitch acceleration for the extreme sea scenarios (Figure 25). For the test with the stationary rotor, where a slack-line event occurred but was not predicted, the platform-pitch acceleration was severely under predicted, as before. However, when a slack-line occurred both in the wave tank and in the numerical simulation, results for platform-pitch acceleration showed considerably better agreement. This supports the suggestion that the physical mechanism exciting the platform in pitch was not captured in the FAST model for most events, but when the excitation mechanism was captured, results for platform response were well predicted. This could, as suggested earlier, be due to the lack of second-order sum-frequency excitation in FAST.

### **Conclusions**

Results presented here confirm that FAST produces meaningful results for simulation of a TLP when a model is carefully calibrated. Considering the current capabilities and observed accuracy presented here for FAST simulations, there is a possibility for large errors in an uncalibrated model, and design of a reliable TLP-supported floating turbine may be more challenging than other concepts currently under consideration. Of particular importance is addressing the challenges in accurately predicting the pitch response of the platform. It is possible that inclusion of second-order hydrodynamics and a dynamic mooring line model will contribute to improving simulation accuracy. This challenge is somewhat unique to the TLP concept, where platform roll, pitch, and heave reside outside of frequencies directly excited by the waves. A better understanding of interaction between tower bending and platform roll/pitch is also likely to improve simulation accuracy. To accomplish this, it is suggested that future tests focus more effort on identifying tower-bending characteristics, improve accuracy of platform-pitch measurements to capture the small pitch values associated with a TLP, and capture data at a higher rate to better resolve behavior of the tower. The need to simulate additional damping in the platform response will likely be reduced if the platform geometry, such as changes in diameter and platform legs, and associated viscous drag are explicitly modeled in all directions. Finally, efforts to compare experimental results to simulations would benefit from a method that is able to directly simulate the experimentally realized wave time history. The lack of this ability is likely a key contributor to the failure to numerically predict some of the slack-line events that occurred experimentally. Overall, the

results are encouraging and show that, even for a relatively light platform subjected to extreme sea states, many design parameters are reasonably predicted by FAST.

## Acknowledgements

The authors thankfully acknowledge the financial support from the U.S. Department of Energy through contract number DE-AC36-08GO28308, DeepCwind Grants DE-EE0002981 and DE-EE0003728, the National Science Foundation through Grant IIP-0917974; and the University of Maine. In addition, the expertise and support of MARIN in conducting the model test is greatly appreciated.

## References

- Bir, G. S. (2005). *User's Guide to BModes; Software for Computing Rotating Beam Coupled Modes*. NREL TP-500-38976, National Renewable Energy Laboratory, Golden, Colorado, USA.
- Brincker, R., Zhang, L., and Andersen, P. (2000). "Modal Identification from Ambient Responses Using Frequency Domain Decomposition." *Proceedings of the 18th international modal analysis conference*, Society for Experimental Mechanics Inc., Bethel, Connecticut, USA, 625-630.
- Coulling, A.J., Goupee, A.J., Robertson, A.N., Jonkman, J.M. and Dagher, H.J. (2013a). "Validation of a FAST Semi-submersible Floating Wind Turbine Model with DeepCwind Test Data." *Journal of Renewable and Sustainable Energy*, in review.
- Coulling, A.J., Goupee, A.J., Robertson, A.N., and Jonkman, J.M. (2013b). "Importance of Second-Order Difference-Frequency Wave-Diffraction Forcing in the Validation of a FAST Semi-Submersible Floating Wind Turbine Model." *Proceedings of the 32nd International Conference on Ocean, Offshore and Arctic Engineering*, American Society of Mechanical Engineers, New York, New York, USA. 1-10
- de Ridder, E. J., Koop, A., and van Doeveren, B. (2011a). *DeepCwind Floating Wind Turbine Model Tests: Volume 3a: Test Data Results – TLP in Mooring System – Draft 30 m*. 24602-1-OB, Maritime Research Institute Netherlands, Wageningen, The Netherlands.
- de Ridder, E. J., Koop, A., and van Doeveren, B. (2011b). *DeepCwind Floating Wind Turbine Model Tests: Volume I: Final Text Report*. 24602-1-OB, Maritime Research Institute Netherlands, Wageningen, The Netherlands.
- Goupee, A. J., Koo, B. J., Lambrakos, K. F., and Kimball, R. W. (2012). "Model Tests for Three Floating Wind Turbine Concepts." *Offshore Technology Conference*, OTC, Richardson, Texas, USA, 1-16.
- Jain, A., Robertson, A. N., Jonkman, J. M., Goupee, A. J., Kimball, R. W., and Swift, A. H. P. (2012). "FAST Code Verification of Scaling Laws for DeepCwind Floating Wind System Tests." *NREL/CP-5000-54221*, National Renewable Energy Laboratory, Golden, Colorado, USA.
- Jonkman, J. M. and Buhl, M. L., Jr. (2005). *FAST User's Guide*. NREL/EL-500-38230, National Renewable Energy Laboratory, Golden, Colorado, USA.
- Jonkman, J., Butterfield, S., Musial, W., and Scott, G. (2009). *Definition of a 5-MW Reference Wind Turbine for Offshore System Development*. NREL/TP-500-38060, National Renewable Energy Laboratory, Golden, Colorado, USA.
- Kim, M. (1991). "Second-Order Sum-Frequency Wave Loads on Large-Volume Structures." *Appl.Ocean Res.*, 13(6), 287-296.
- Koo, B., Goupee, A. J., Lambrakos, K., and Kimball, R. W. (2012). "Model Tests for a Floating Windturbine on Three Different Floaters." *Proceedings of the 31st International Conference on Ocean, Offshore and Arctic Engineering*, American Society of Mechanical Engineers, New York, New York, USA, 1-11.
- Martin, H. R. (2011). *Development of a Scale Model Wind Turbine for Testing of Offshore Floating Wind Turbine Systems*. Masters of Science thesis, The University of Maine, Orono, Maine, USA.
- Naess, A., and Ness, G. (1992). "Second-Order, Sum-Frequency Response Statistics of Tethered Platforms in Random Waves." *Appl.Ocean Res.*, 14(1), 23-32.

Stewart, G., Lackner, M., Robertson, A., Jonkman, J., and Goupee, A. (2012). "Calibration and Validation of a FAST Floating Wind Turbine Model of the DeepCwind Scaled Tension-Leg Platform." *NREL/CP-500-54822*, National Renewable Energy Laboratory, Golden, Colorado, USA.

WAMIT Inc. (2006). *WAMIT User Manual*. WAMIT, Inc., Chestnut Hill, Massachusetts, USA.

## Tables

Table 1 – Properties of the Tested Turbine

Property	Value
Rotor Orientation, Configuration	Upwind, 3 Blades
Control	Variable Speed and Pitch
Rotor, Hub Diameter	126 m, 3 m
Hub Height	90 m
Freeboard to Tower Base	10 m
Overhang, Shaft Tilt, Precone	10.58 m, 0°, 0°
Rotor Mass	122,220 kg
Nacelle Mass	274,940 kg
Tower Mass	302,240 kg

Table 2 – Platform Properties

Property	Value
Legs Configuration	3 radially at 120°
Radius to Fairlead	30 m
Draft of Fairlead	28.5 m
Mass	661,600 kg
Displacement	2,840,000 kg
Platform Draft	30 m
Water Depth	200 m
Radius to Anchor	30 m

Table 3 – Modal Frequencies as Identified and Predicted for the Tuned FAST Model

Mode Description	Orientation	Experimental Frequency	Model Frequency
	(-)	(Hz)	(Hz)
Platform Surge	Fore-Aft	0.0259	0.0267
Platform Sway	Side-to-Side	0.0259	0.0267
Platform Yaw	Yaw	-	0.0548
Platform Pitch	Pitch	0.268	0.267
Platform Roll	Roll	0.276	0.279
Platform Heave	Vertical	0.863	0.864
Tower 1 <sup>st</sup> Bending	Fore-Aft	1.631	1.300
Tower 1 <sup>st</sup> Bending	Side-to-Side	1.511	1.318
Tower 2 <sup>nd</sup> Bending	Side-to-Side	3.328	3.118
Tower 2 <sup>nd</sup> Bending	Fore-Aft	3.535	3.236

Table 4 – Adjustments for Platform DOFs

DOF	Damping		Stiffness (Linear)
	Linear	Quadratic	
Surge	$7 \times 10^4$ Ns/m	$2.7 \times 10^5$ Ns <sup>2</sup> /m <sup>2</sup>	$8.5 \times 10^3$ N/m
Sway	$2 \times 10^3$ Ns/m	$8.0 \times 10^5$ Ns <sup>2</sup> /m <sup>2</sup>	$8.5 \times 10^3$ N/m
Heave	0 Ns/m	$2.5 \times 10^6$ Ns <sup>2</sup> /m <sup>2</sup>	0 N/m
Roll	$4 \times 10^8$ Ns/rad	$9.0 \times 10^{10}$ Ns <sup>2</sup> /rad <sup>2</sup>	0 N/rad
Pitch	$4 \times 10^8$ Ns/rad	$9.0 \times 10^{10}$ Ns <sup>2</sup> /rad <sup>2</sup>	0 N/rad
Yaw	$4.5 \times 10^8$ Ns/rad	$3.6 \times 10^9$ Ns <sup>2</sup> /rad <sup>2</sup>	$-1.3 \times 10^7$ N/rad

Table 5 – Summary of Regular Wind Tests

Wind Speed Reported by MARIN	Wind Speed in FAST Simulation	Blade Pitch	Rotor Speed
(m/s)	(m/s)	(deg)	(RPM)
7.0	6.97	6.4	4.95
9.0	8.51	6.4	5.66
11.4	10.69	6.4	7.78
16.0	15.34	6.4	9.19
21.0	20.75	6.4	12.73
30.5	29.04	85	0.0

Table 6 – Summary of Regular Wave Sea States

Wave Period	Wave Height
(s)	(m)
7.5	1.92
12.1	7.58
14.3	7.14
20.0	7.57
12.1	10.30
14.3	10.74
20.0	11.12

Table 7 – Summary of Combined Wave and Wind Tests for Normal Conditions

Wind Speed	Blade Pitch	Rotor Speed	H <sub>s</sub>	T <sub>p</sub>	γ*
(m/s)	(deg)	(RPM)	(m)	(s)	(-)
7.0	6.4	4.95	2.0	7.5	2.0
9.0	6.4	5.66	2.0	7.5	2.0
11.4	6.4	7.78	2.0	7.5	2.0
11.4	6.4	7.78	7.1	12.1	2.2
16.0	6.4	9.19	7.1	12.1	2.2
21.0	6.4	12.73	7.1	12.1	2.2

\*γ is the JONSWAP peak-shape parameter

Table 8 – Summary of Combined Wave and Wind Tests for Extreme Conditions

<b>Wind Speed</b>	<b>Blade Pitch</b>	<b>Rotor Speed</b>	<b>H<sub>s</sub></b>	<b>T<sub>p</sub></b>	<b>γ</b>
<b>(m/s)</b>	<b>(deg)</b>	<b>(RPM)</b>	<b>(m)</b>	<b>(s)</b>	<b>(-)</b>
21.0	6.4	12.73	10.5	14.3	3.0
30.5	85	0.0	10.5	14.3	3.0

## Figures

Figure 1 – Experimental Test Configuration. *Photo by Andrew Goupee, University of Maine*

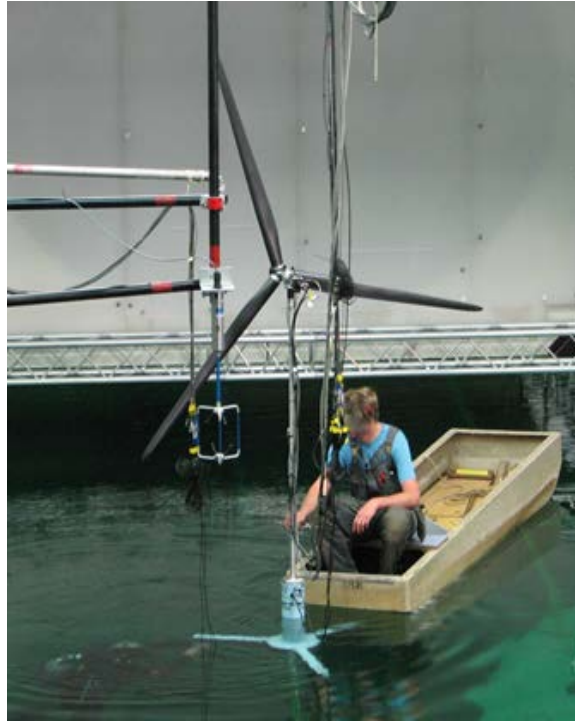


Figure 2 – Definition of Axes

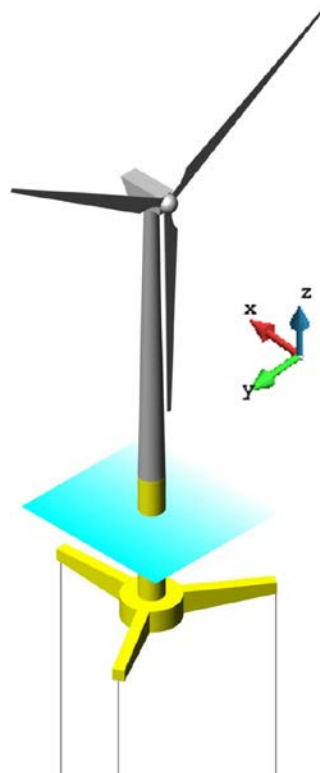


Figure 3 – Location of Instrumentation (de Ridder et al. 2011a)

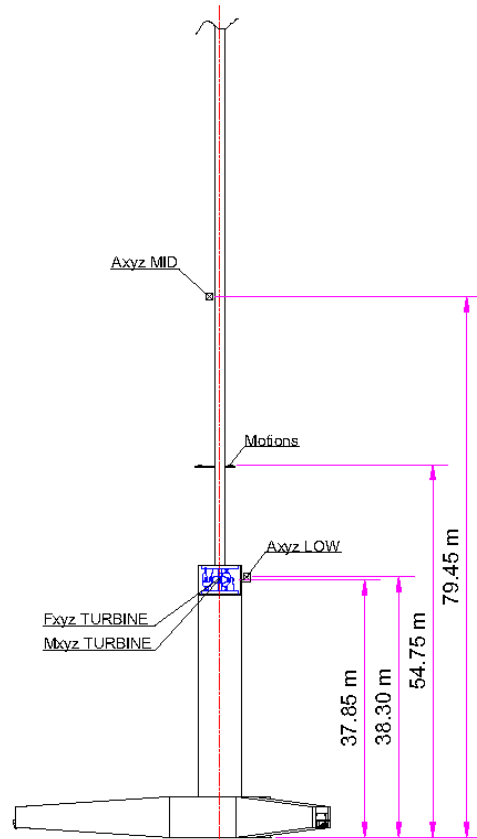


Figure 4 – Comparison of Experimental and Numerical Surge Response After FAST Calibration

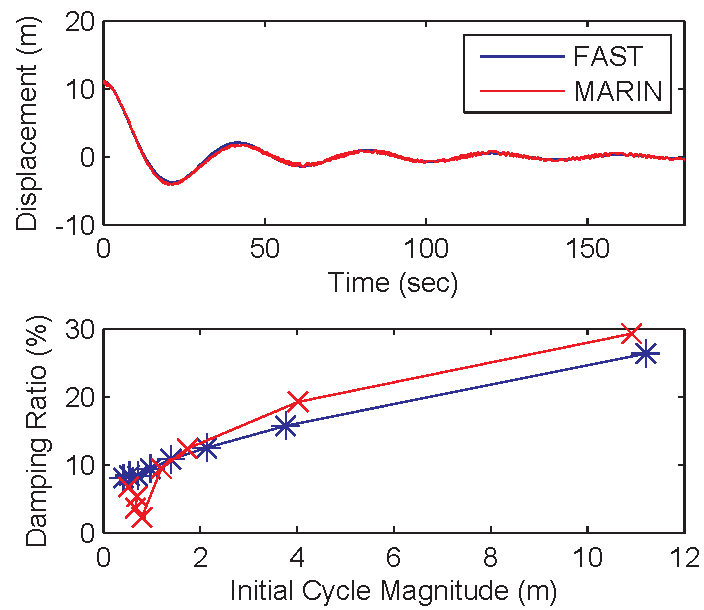


Figure 5 – Conceptual Adaption of Mode Shape

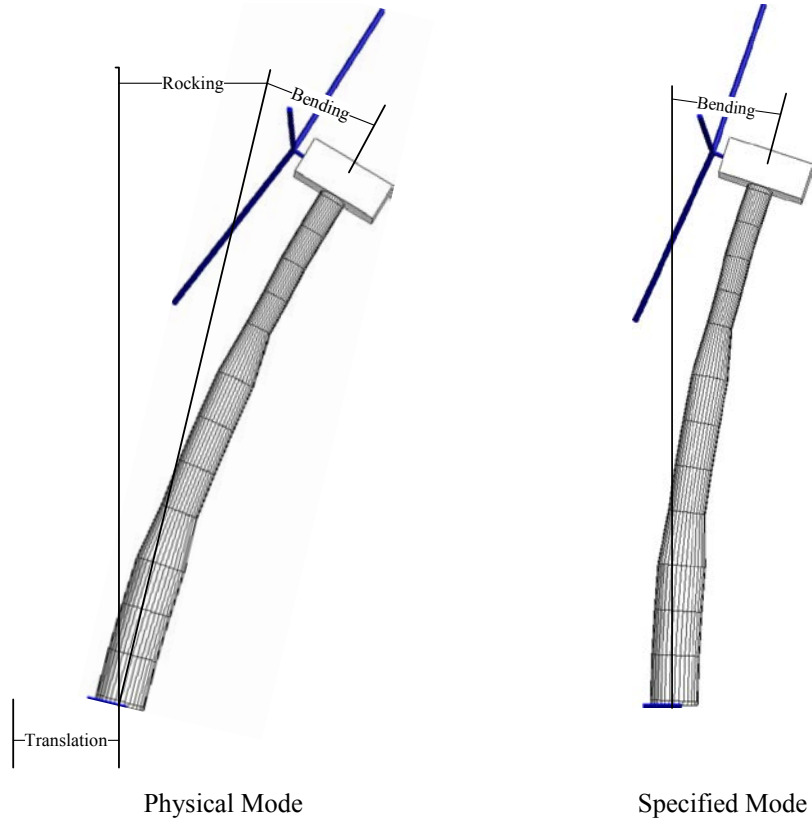


Figure 6 – Turbine Pitch Mode Shape Predicted by FAST at 0.267 Hz

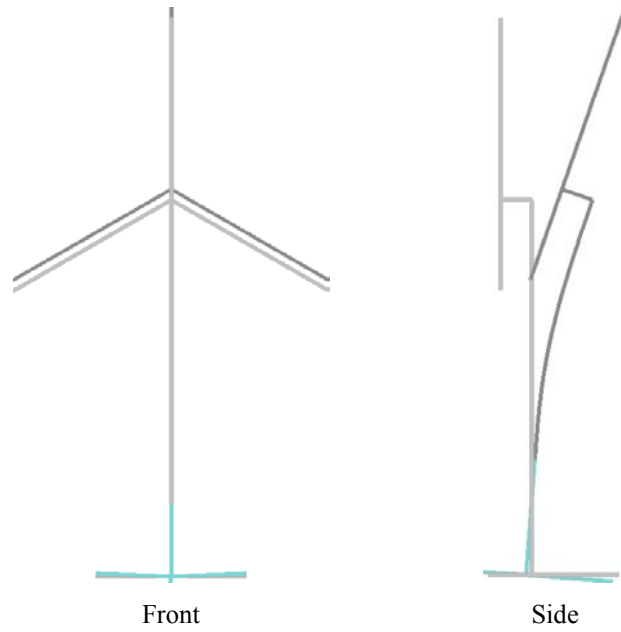


Figure 7 – Turbine 1<sup>st</sup> Tower Fore-Aft Bending Mode Shape Predicted by FAST at 1.300 Hz

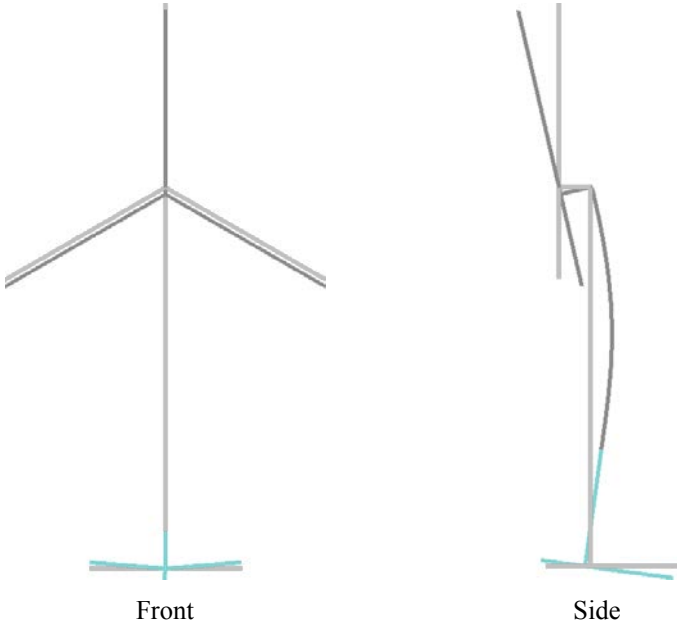


Figure 8 – Turbine 2<sup>nd</sup> Tower Fore-Aft Bending Mode Shape Predicted by FAST at 3.236 Hz

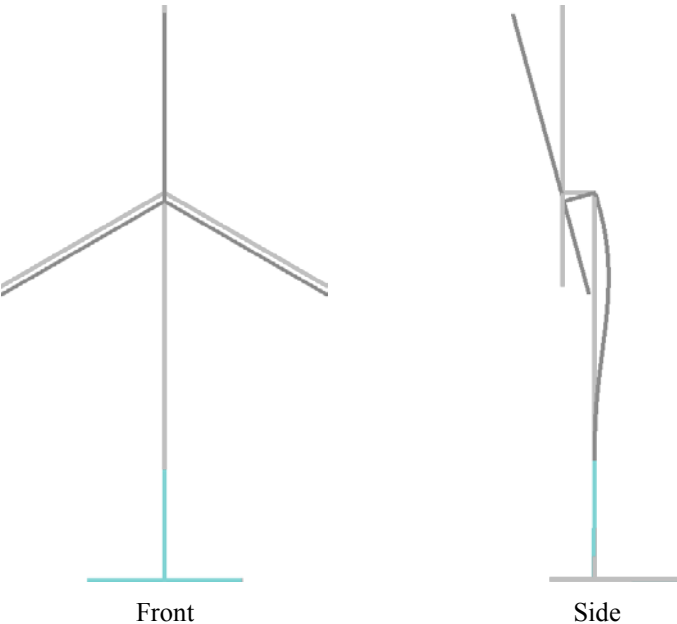


Figure 9 – Platform-Surge Response for Regular Wind Tests

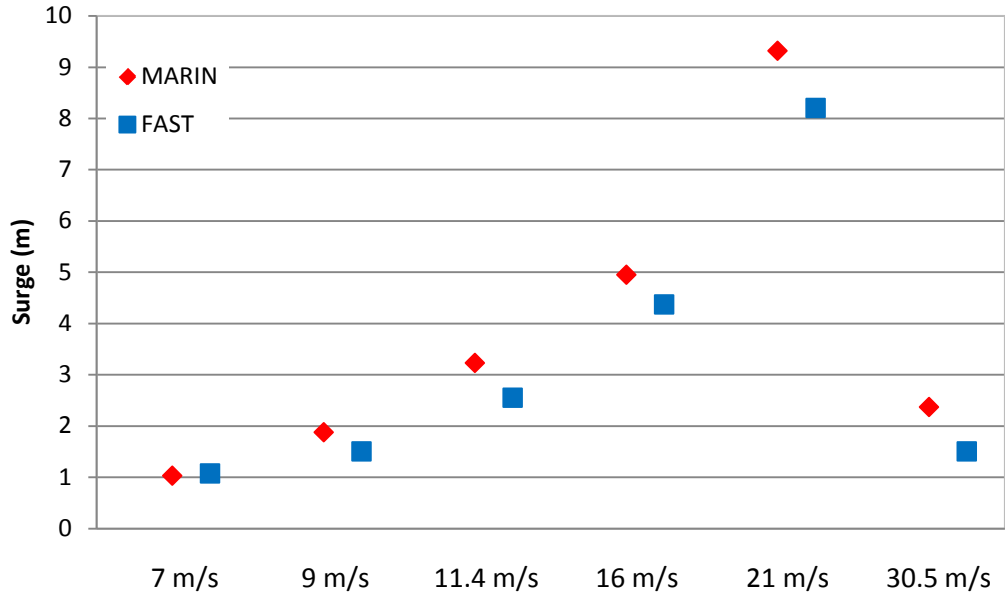


Figure 10 – Tower-Base Bending Moment Response for Regular Wind Tests

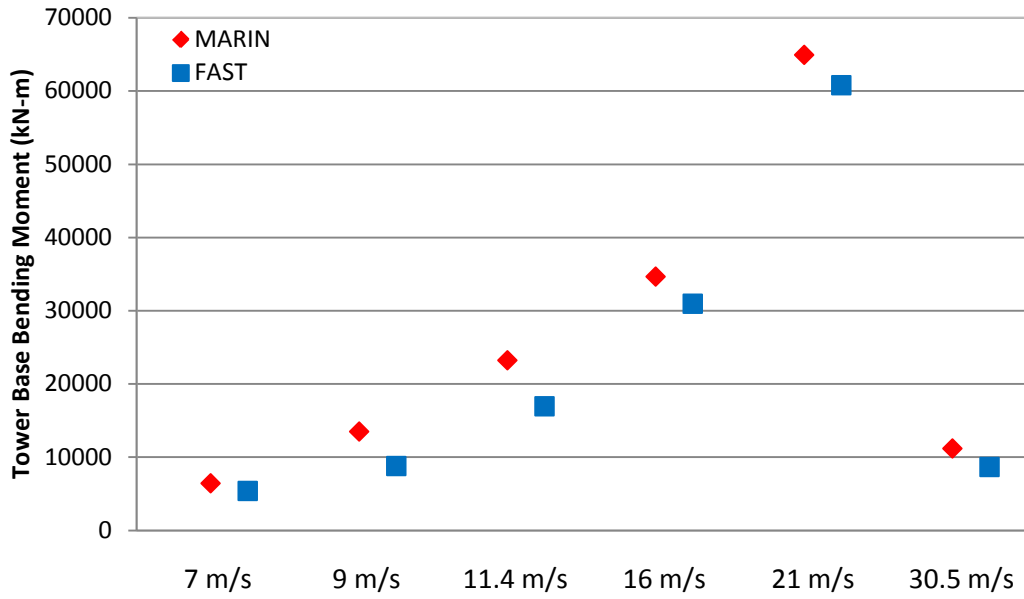


Figure 11 – Platform-Surge Statistics for Regular Wave Tests

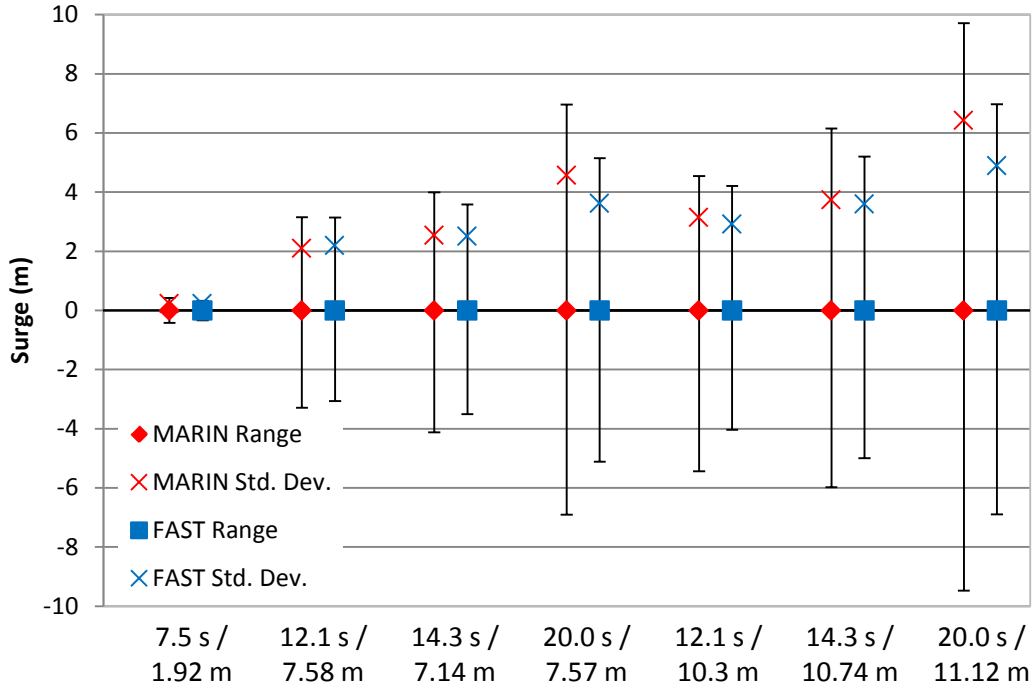


Figure 12 – Platform-Pitch Acceleration for Regular Wave Tests

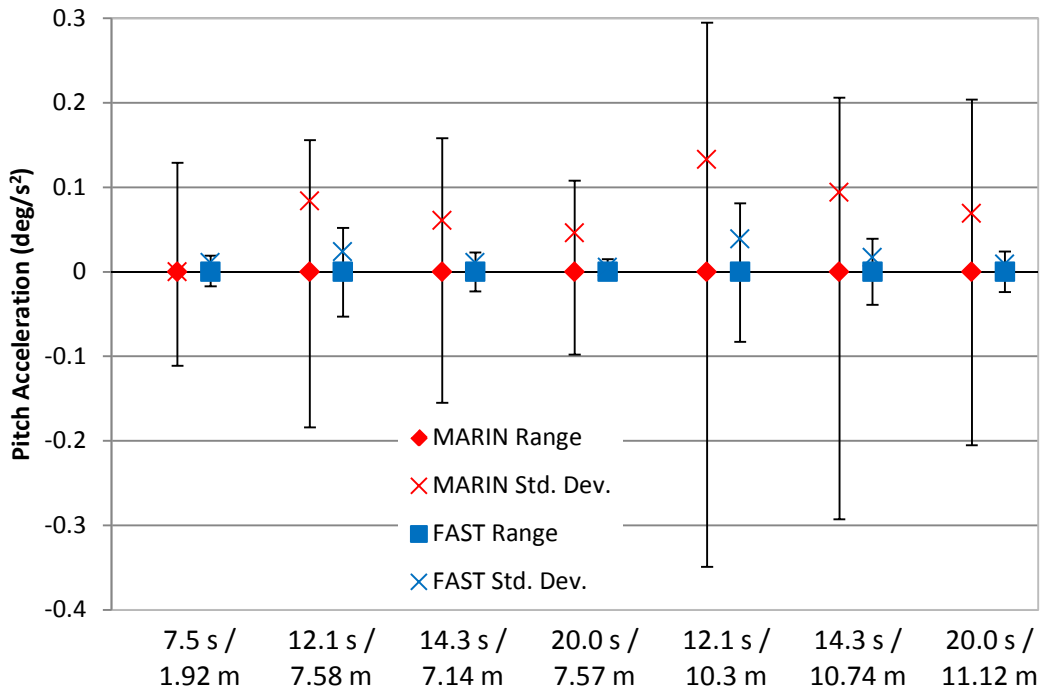


Figure 13 – Illustrative Results for 7.5-s Period, 1.92-m Height Regular Waves

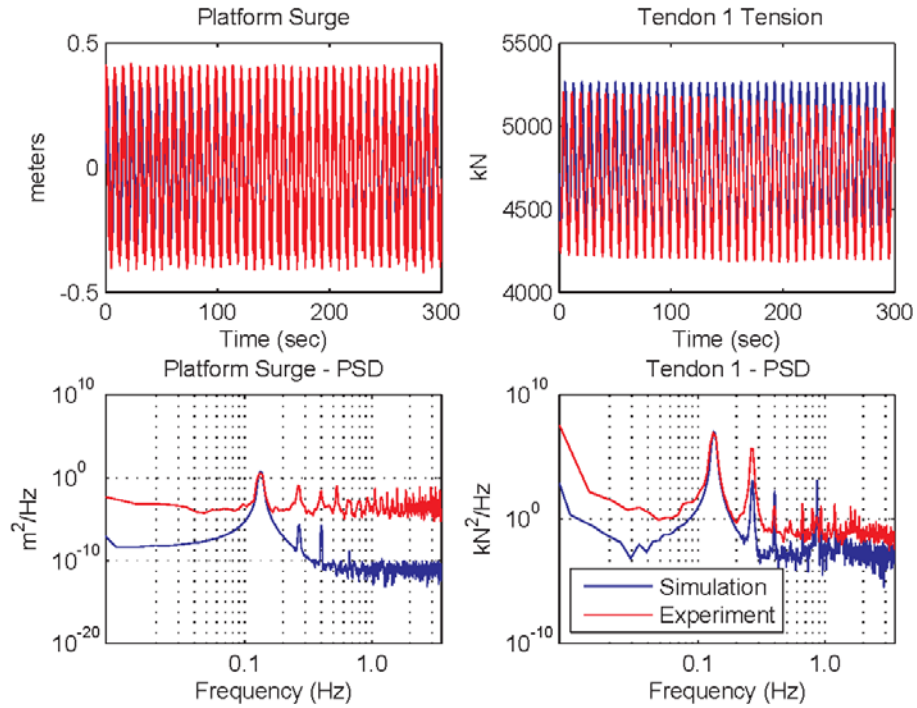


Figure 14 – Illustrative Results for 7.5-s Period, 1.92-m Height Regular Waves

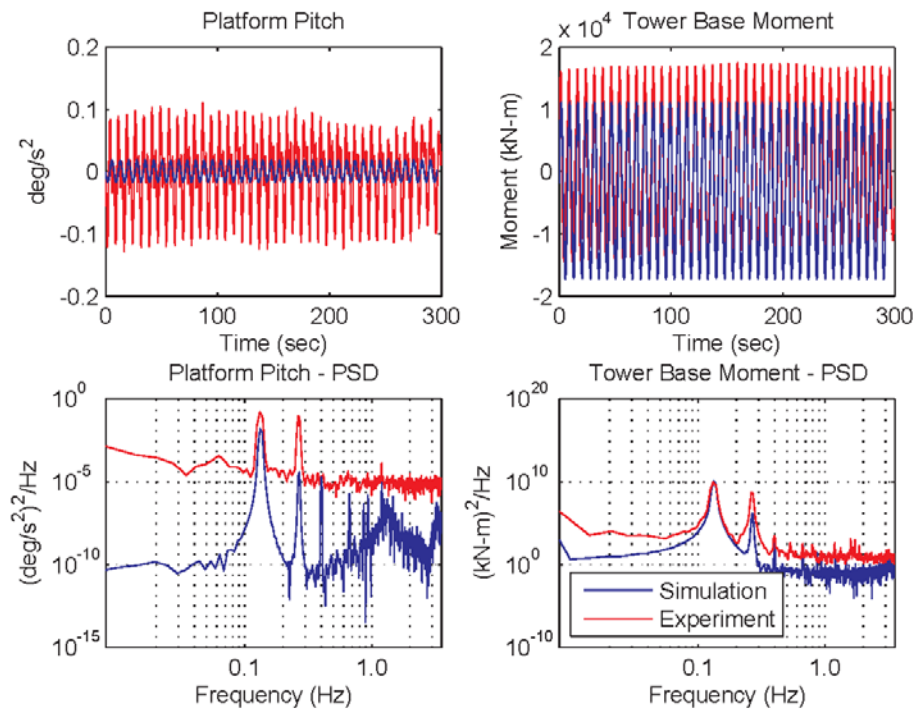


Figure 15 – Summary of Realized Wave Statistics for Combined Wave and Wind Tests

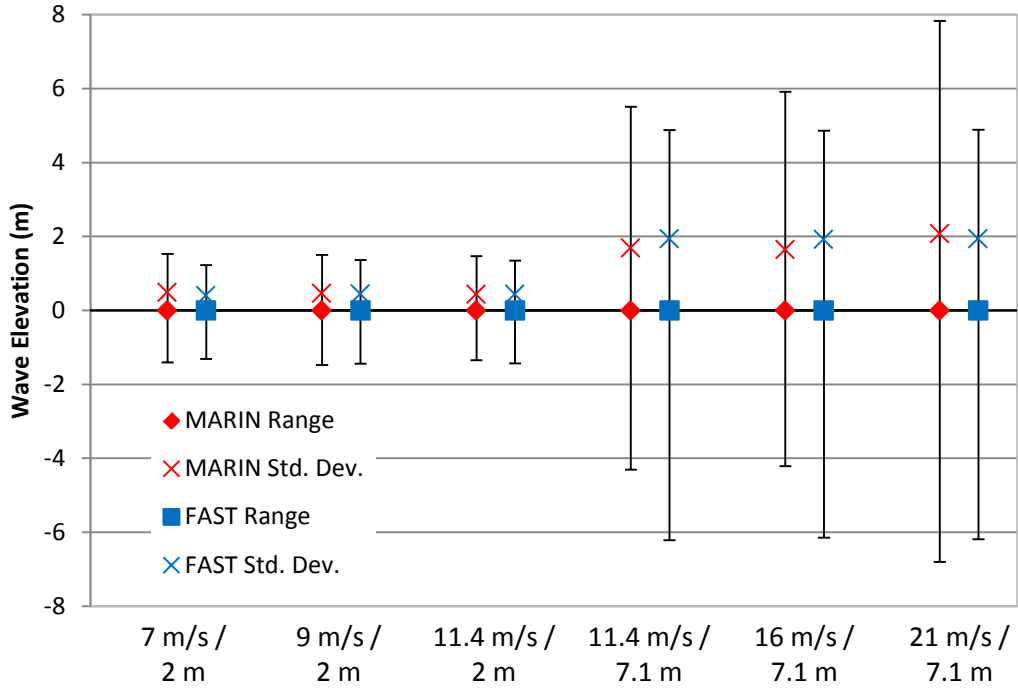


Figure 16 – Tendon 1 Tension Statistics for Combined Wave and Wind Tests

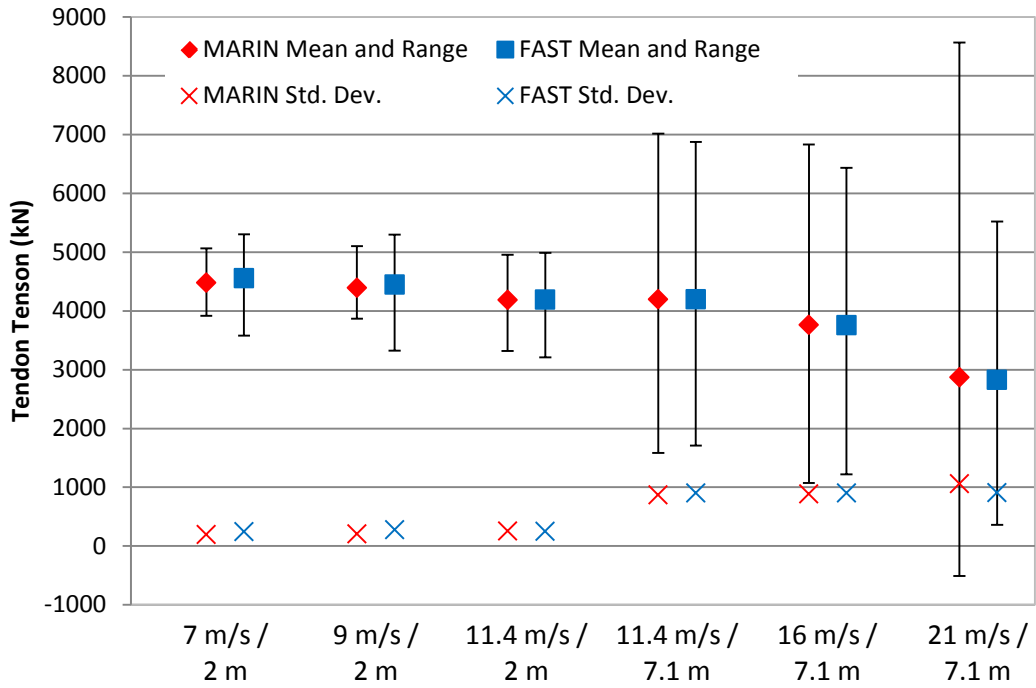


Figure 17 – Platform-Pitch Acceleration Statistics for Combined Wave and Wind Tests

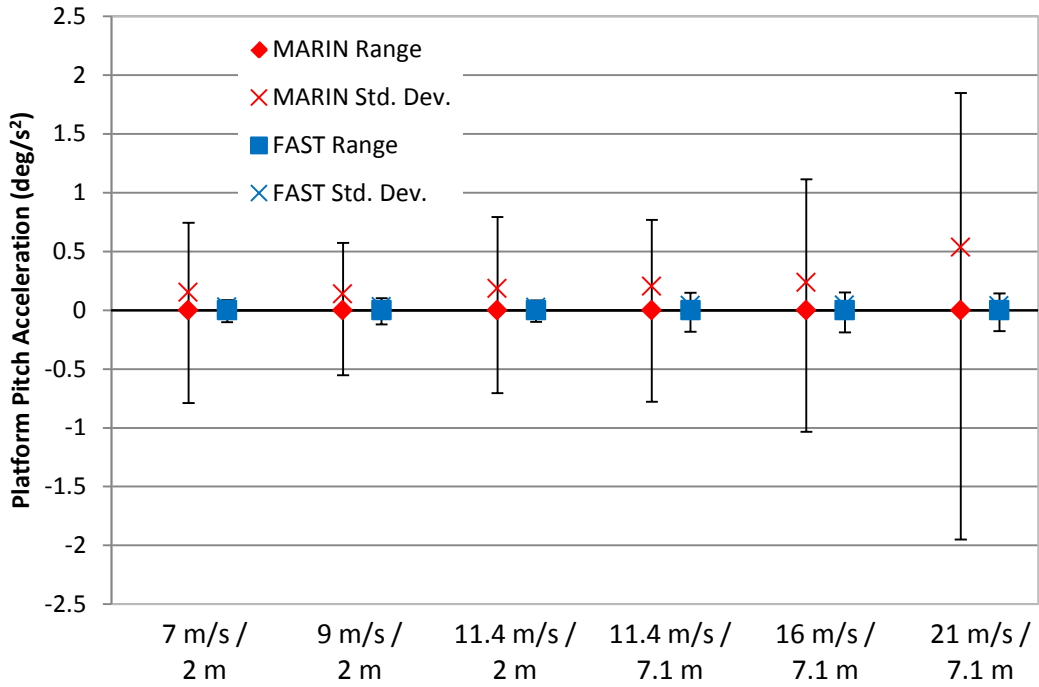


Figure 18 – Comparison of Waves for Wind Speed of 11.4 m/s and JONSWAP Waves ( $T_p = 12.1$  s /  $H_s = 7.1$  m)

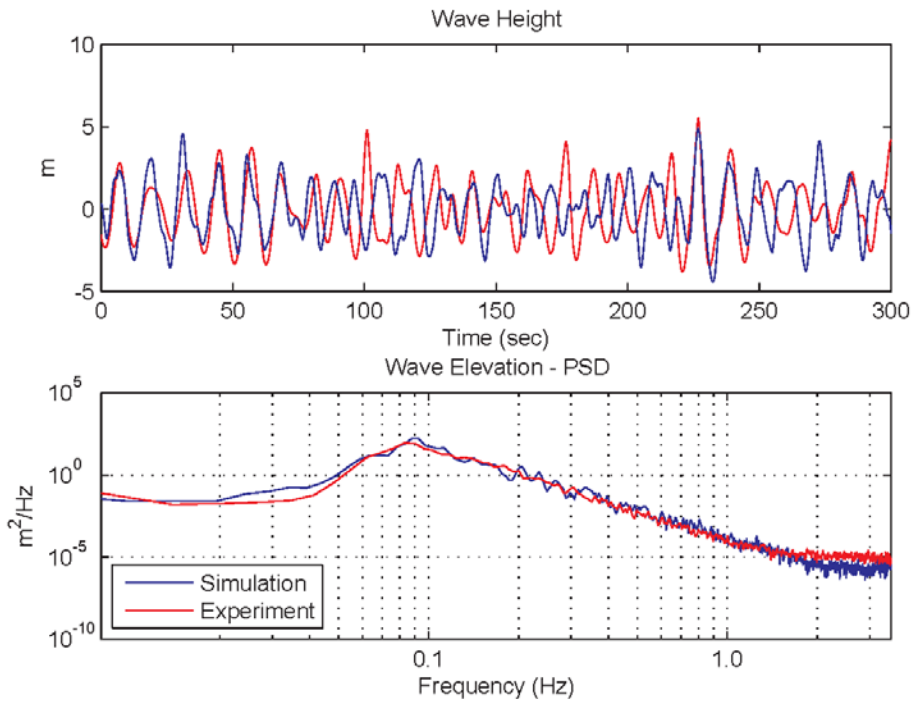


Figure 19 – Illustrative Results for Operating in 11.4-m/s Wind with 7.1-m Significant Wave Height JONSWAP Waves

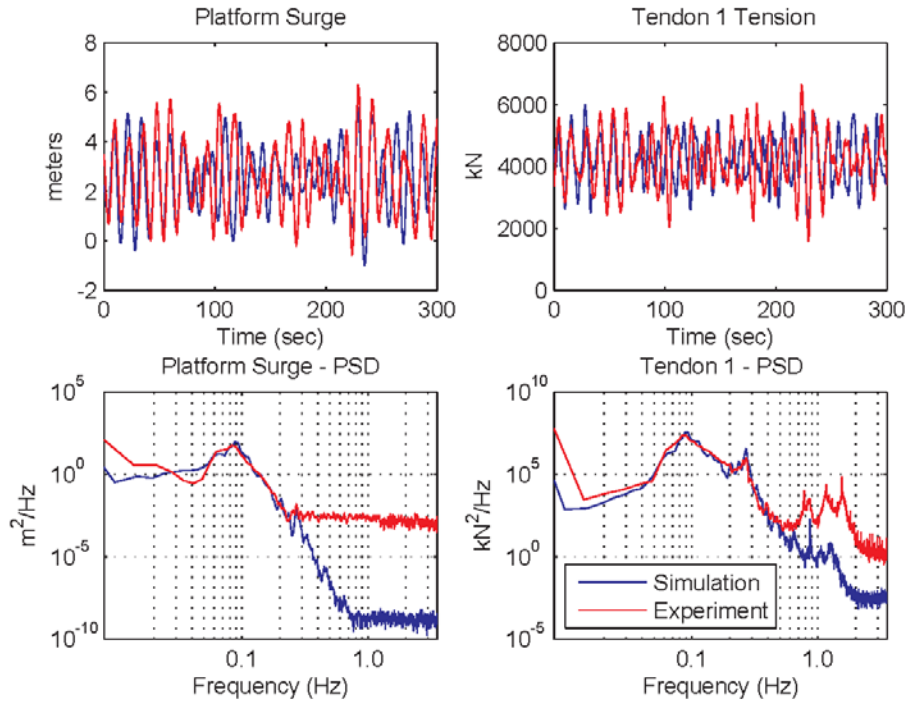


Figure 20 – Illustrative Results for Operating in 11.4-m/s Wind with 7.1-m Significant Wave Height JONSWAP Waves

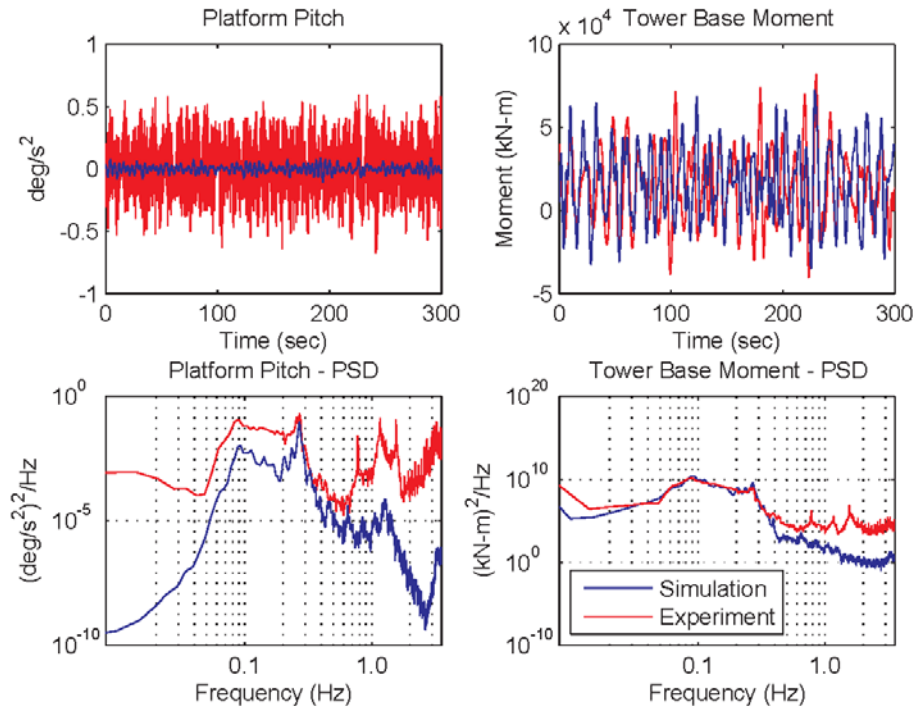


Figure 21 – Summary of Realized Wave Statistics for Combined Wave and Wind Tests for Extreme Conditions

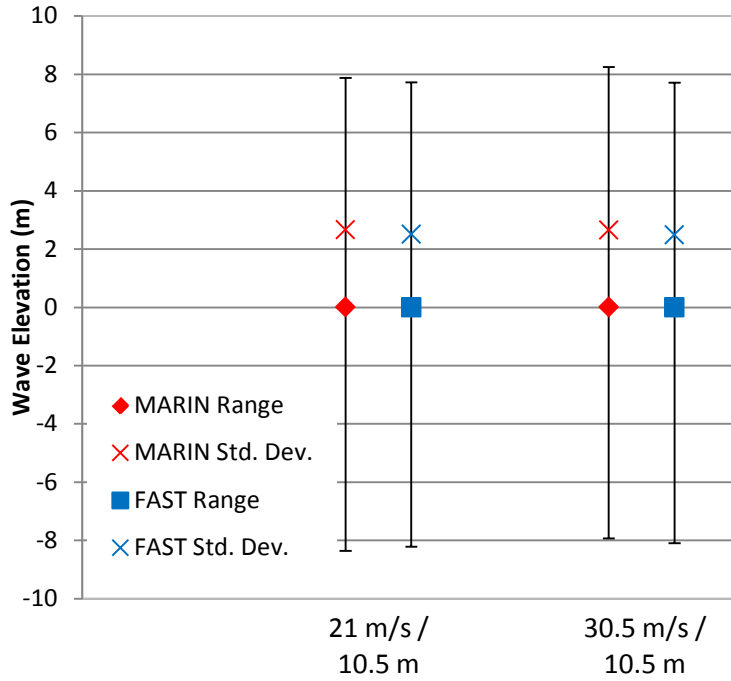


Figure 22 – Tendon 1 Tension Statistics for Combined Wave and Wind Tests for Extreme Conditions

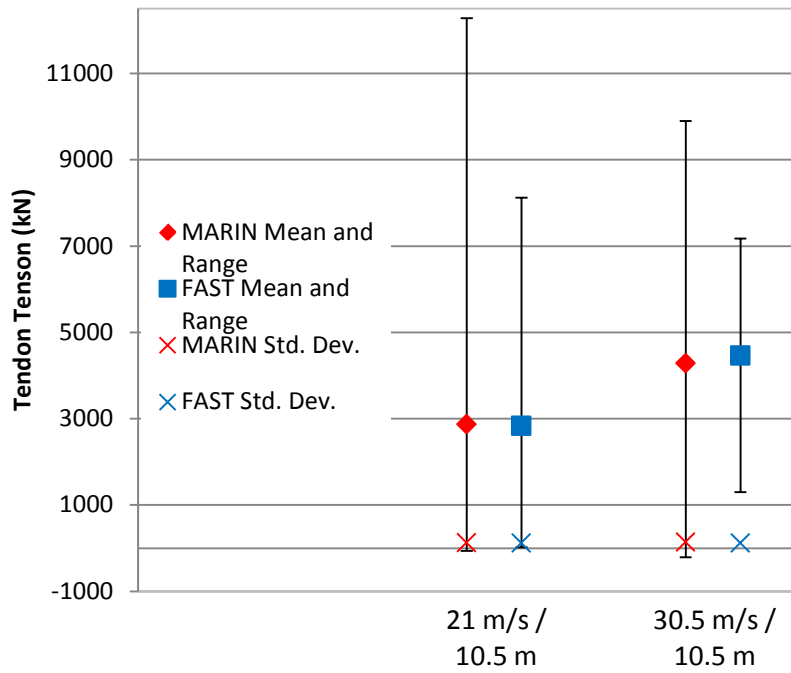


Figure 23 – Illustrative Results for Slack-Line Event While Operating in Extreme Conditions

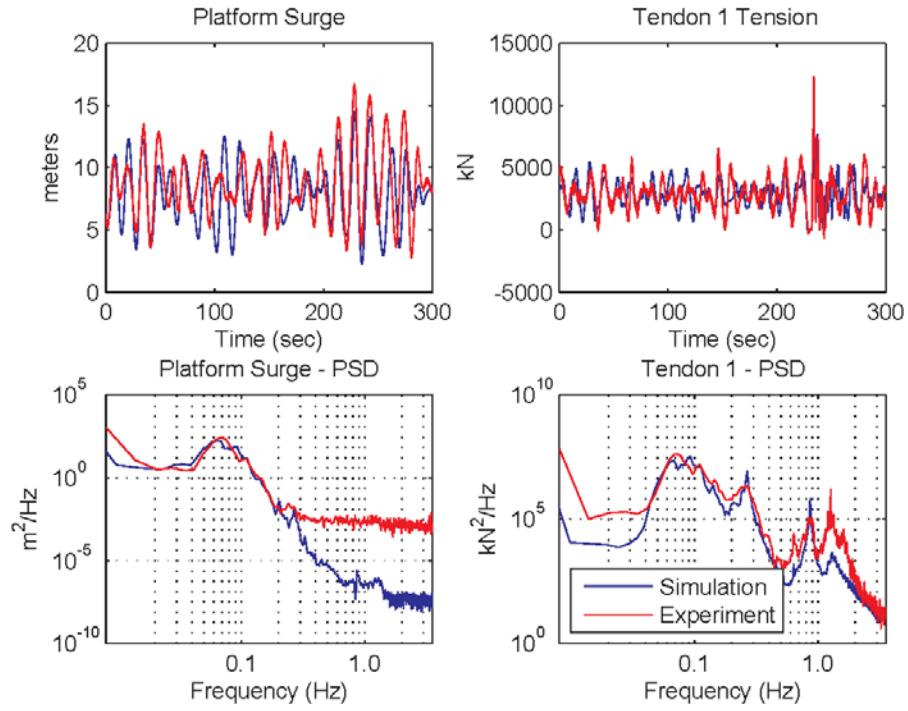


Figure 24 – Illustrative Results for Slack-Line Event While Operating in Extreme Condition

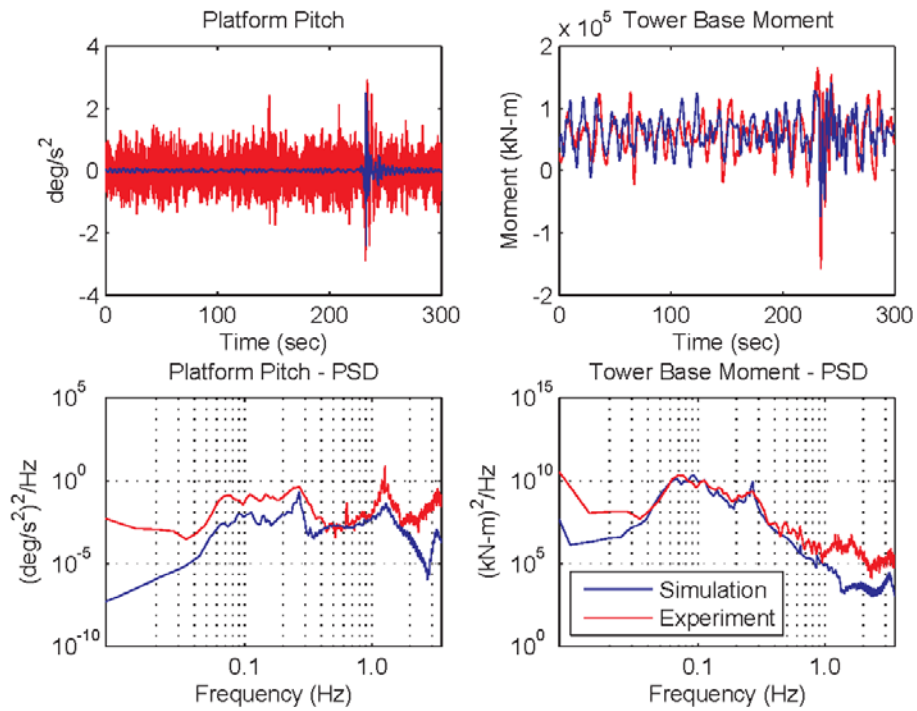


Figure 25 – Platform-Pitch Acceleration Statistics for Combined Wave and Wind Tests for Extreme Conditions

